



## Full paper/Mémoire

# Green, inexpensive, and fast conversion of sulfides to sulfoxides by multiusable Mo(VI) macrocyclic Schiff base complex supported on $\text{Fe}_3\text{O}_4$ nanoparticles in solvent-free conditions

Abolfazl Bezaatpour\*, Fatemeh Payami, Habibollah Eskandari

Department of Chemistry, Faculty of Basic Science, University of Mohaghegh Ardabili, 179, Ardabil, Iran

## ARTICLE INFO

## Article history:

Received 8 May 2017

Accepted 13 July 2017

Available online xxxx

## Keywords:

Macrocyclic ligand

Oxidation

Nanocatalyst

Molybdenum

Solvent-free conditions

## ABSTRACT

In the present study, the macrocyclic-based Mo(VI) Schiff base complex was harbored on  $\text{Fe}_3\text{O}_4$  nanoparticles and characterized by X-ray powder diffraction, scanning electron microscope, energy-dispersive X-ray spectroscopy, infrared spectroscopy, transmission electron microscopy, vibrating sample magnetometry, diffuse reflectance spectra, and atomic absorption spectroscopy. Separable nanocatalyst was tested under solvent-free conditions for the oxidation of methyl phenyl sulfide, diphenyl sulfide, benzyl phenyl sulfide, dipropyl sulfide, dibutyl sulfide, dimethyl sulfide, bis (4-hydroxyphenyl) sulfide, diallyl sulfide, and benzothiophene using  $\text{H}_2\text{O}_2$  (30% in water) as green oxidant. This catalyst is very efficient for thioanisole oxidation with 100% conversion in 3 min. We were able to separate the nanocatalyst magnetically using external magnetic field and to apply the catalyst at least six consecutive times without a significant decrease in conversion. Remarkable and excellent turnover frequency of the catalyst was obtained to oxidize the thioanisole ( $526,000 \text{ h}^{-1}$ ), dimethyl sulfide ( $526,000 \text{ h}^{-1}$ ), diallyl sulfide ( $526,000 \text{ h}^{-1}$ ), dibutyl sulfide ( $521,000 \text{ h}^{-1}$ ), and dipropyl sulfide ( $500,000 \text{ h}^{-1}$ ). The prepared nanocatalyst has been beneficial in catalytic activity, selectivity, reaction time, and reusability with easy separation.

© 2017 Académie des sciences. Published by Elsevier Masson SAS. All rights reserved.

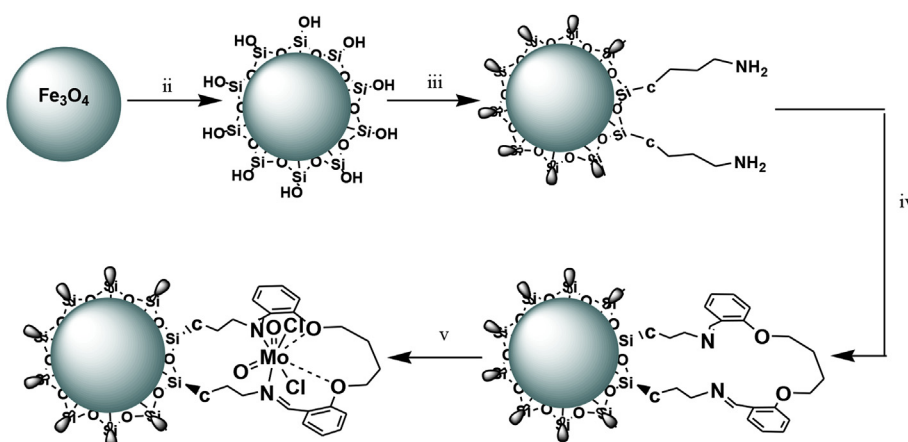
## 1. Introduction

Over the past two decades, the oxidation of sulfides to sulfoxides and sulfones gives beneficial starting chemical materials [1–5]. Sulfoxides are the major chemical intermediates to synthesize valuable chemicals, including medications [6,7] and antifungal agents [8,9], and also can play a role in the activation of enzymes. Numerous recent reports are available on the conversion of sulfides into sulfoxides using transition metal complexes [10–13], especially with Mo complexes [14–17]. The Mo(VI)

complexes have been used intensively as catalysts for selective oxidation of organic compounds [18–20]. There are some key advantages for solvent-free reactions, such as significant contributions to protect the environment, health of people, high cost efficiency, and waste reduction [21]. According to previous reports, aqueous solution of hydrogen peroxide (30%) is one of the greenest oxidants, because it is cheap, nontoxic, and environmentally benign without waste products, so that water is the only residue [22–24]. A homogeneous catalyst recovering from a reaction mixture is often difficult and costs high, as well as is associated with additional wastes. Furthermore, insufficient chemical and thermal stability, the active metal leaching into the solvent, and catalyst recycling remain a

\* Corresponding author.

E-mail address: [bezaatpour@uma.ac.ir](mailto:bezaatpour@uma.ac.ir) (A. Bezaatpour).



**Scheme 1.** Preparation of the heterogeneous nanocatalyst. (i)  $K_2CO_3$ /DMF, (ii) tetraethoxysilane/EtOH, (iii) APTMS/EtOH, (iv) 1,4-bis(2-carboxyaldehyde phenoxy) butane + stirring at  $70\text{ }^{\circ}\text{C}$  for 48 h/EtOH, and (v)  $MoO_2Cl_2$ (DMF)<sub>2</sub>/EtOH.

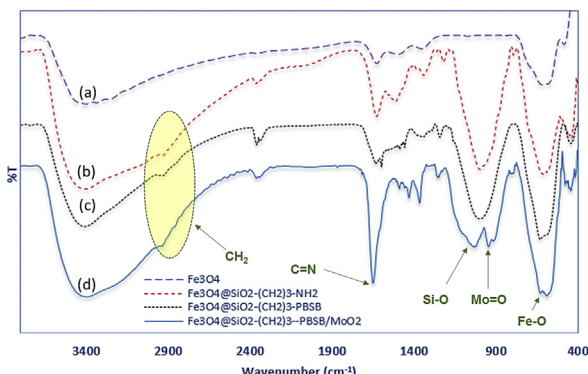


**Fig. 1.** FT-IR spectrum of (a)  $Fe_3O_4$  NP, (b)  $Fe_3O_4@SiO_2-(CH_2)_3-NH_2$ , (c)  $Fe_3O_4@SiO_2-(CH_2)_3-PBSB$ , (d)  $Fe_3O_4@SiO_2-(CH_2)_3-PBSB/MoO_2$ .

scientific challenge [25]. Replacement of a homogeneous oxidation catalyst with environmental friendly heterogeneous catalyst may be promising address for such problems [26]. Accordingly, metal complex supporting has been the

basic research subject in the catalytic fields [18,27–29]. A main idea for supporting of metal complexes is to anchor the metal complex onto a large surface area of inorganic materials, such as zeolite and metal oxide [30–36]. Nowadays, magnetite nanoparticles (NPs) have been recruited because of their unique properties, including the large surface area, low toxicity, separate-ability, and biocompatibility [37–43]. Magnetic separation renders the recycling of catalysts from the solution by external magnetic fields much easier than filtration and centrifugation. Following our previous review on catalytic activity of Schiff base complexes [19,27,30,44–46], herein we report the anchoring of novel *cis*-dioxomolybdenum(VI) macrocyclic Schiff base complex by a reaction of 1,4-bis(2-carboxyaldehyde phenoxy) butane,  $MoO_2Cl_2$ (DMF)<sub>2</sub> and amino-modified magnetite NPs. The novel nanocatalyst ( $Fe_3O_4@Si(CH_2)_3-PBSB/MoO_2$ ) (PBSB: propylbromo Schiff base) was characterized using infrared (IR) spectroscopy, scanning electron microscope (SEM), transmission electron microscopy, diffuse reflectance spectra (DRS), vibrating sample magnetometry, energy-dispersive X-ray (EDX)

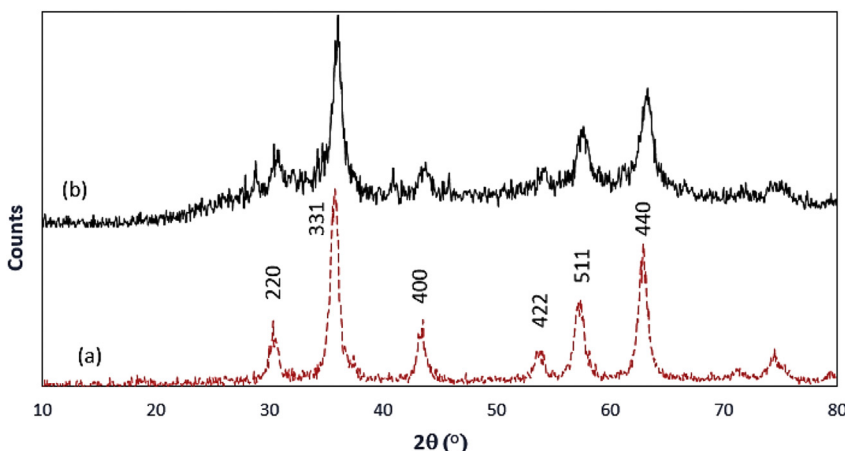


**Fig. 2.** Pattern of XRD, (a) magnetite NPs, (b)  $Fe_3O_4@SiO_2-(CH_2)_3-PBSB/MoO_2$ .

spectroscopy, and X-ray powder diffraction (XRD) techniques and tested for methyl phenyl sulfide, diphenyl sulfide, benzyl phenyl sulfide, dipropyl sulfide, dibutyl sulfide, dimethyl sulfide, bis(4-hydroxyphenyl) sulfide, diallyl sulfide, and benzothiophene with  $H_2O_2$  (30% aqueous) as oxidant. The reusability of  $Fe_3O_4@Si$ -APFSB-MoO<sub>2</sub> (APFSB: aminopropyl phenoxybutane Schiff base) was also studied within the oxidation of methyl phenyl sulfide with  $H_2O_2$  (30% aqueous) under solvent-free conditions for six times.

## 2. Experimental section

### 2.1. Materials and instruments

Methyl phenyl sulfide, diphenyl sulfide, benzyl phenyl sulfide, dipropyl sulfide, dibutyl sulfide, dimethyl sulfide, bis(4-hydroxyphenyl) sulfide, diallyl sulfide, benzothiophene, 1,4-dibromobutane, 2-hydroxybenzaldehyde, *N,N*'-dimethylformamide, ferrous chloride, ferric chloride, 3-aminopropyltrimethoxysilane (APTMS), and ammonia (25%[w/w]) were purchased from Merck Chemical Company. Proton nuclear magnetic resonance spectra were recorded using a Bruker NMR 400 (400 MHz) spectrophotometer in a  $CDCl_3$  solvent. CHNS analyses were performed using an Elemental Analyzer CHNSO-A PE 2400 series II system. Atomic absorption analysis was carried out on an Analytik Jena atomic absorption spectrometry. Analysis of the oxidation products was determined by gas chromatography (GC) using Agilent 7890 A with a capillary column and flame ionization detector. Column temperature was programmed between 180 and 200 °C with 2 °C/min rate.

$N_2$  was used as a carrier gas at a flow rate of 20 mL/min. IR spectra were obtained using a Fourier transform infrared (FT-IR) spectrometer spectomrx 1 in KBr pellets over the range of 4000–400  $cm^{-1}$ . Vibrating sample magnetometer (VSM) was recorded with MDKF-FORC/VSM (Mehnatis-Daghighe-Kashan Co.). DRS data were recorded by Scinco 4100 in the range 200–900 nm using barium sulfate as reference. The powder small angle XRD studies were performed using Philips X'Pert with  $Cu K\alpha$  radiation ( $k = 1.54 \text{ \AA}$ ). Surface morphology and distribution of NPs were investigated using LEO 1430 VP scanning electron microscopy.

### 2.2. Preparation of $Fe_3O_4@SiO_2-(CH_2)_3NH_2$

$Fe_3O_4$  NPs and  $Fe_3O_4@SiO_2$  were prepared according to chemical coprecipitation method given in the literature [39,47,48]. To this end, 1.25 g of  $FeCl_2 \cdot 4H_2O$  and 3.40 g of  $FeCl_3 \cdot 6H_2O$  were dissolved in 100 mL deionized water under nitrogen gas at 60 °C, and then 6 mL of 25% ammonia was added and stirred for 45 min. Next, the magnetite precipitates were separated and washed with water and ethanol several times. For preparation of  $Fe_3O_4@SiO_2$ , 0.145 g of magnetic NPs were dispersed under ultrasonification for 30 min in the presence of  $N_2$  atmosphere.  $H_2O$  (5 mL), ammonia (3 mL), and TEOS (0.4 mL) were added to the mixture and stirred for 5 h at room temperature. Afterward, the obtained solid was separated and washed several times with ethanol and water and dried under vacuum at room temperature. To the suspension of  $Fe_3O_4@SiO_2$  (0.5 g) in ethanol (50 mL) was added dropwise

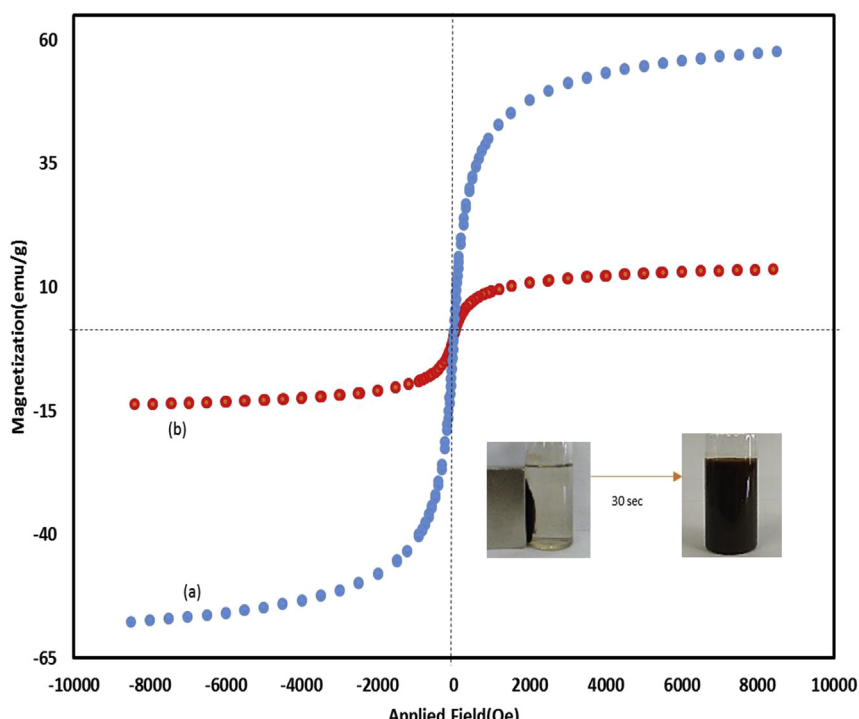


Fig. 3. Magnetization response of (a) magnetite NPs and (b)  $Fe_3O_4@SiO_2-(CH_2)_3-PBSB/MoO_2$  at 25 °C.

the APTMS (2.5 mL) dissolved in 50 mL ethanol. After stirring the mixture at 70 °C for 12 h, the aminated magnetic NPs were collected with external magnetic field and washed with water three times, FT-IR (KBr,  $\text{cm}^{-1}$ ): 3406 [ $\nu(\text{O}-\text{H})$ ], 2924 [ $\nu(\text{C}-\text{H})$  aliphatic], 998 [ $\nu(\text{Si}-\text{O})$ ], 610 [ $\nu(\text{Fe}-\text{O})$ ].

### 2.3. Synthesis of 1,4-bis(2-carboxyaldehyde phenoxy)butane

1,4-Bis(2-carboxyaldehyde phenoxy)butane was synthesized in accordance with İlhan et al. [49]; thus, 1,4-dibromobutane (1.08 g, 5 mmol) was dissolved in 5 mL of

dimethylformamide and then was added dropwise to a solution of 2-hydroxybenzaldehyde (1.22 g, 10 mmol) and potassium carbonate (0.691 g, 5.0 mmol) in dimethylformamide (30 mL). The mixture was refluxed for 15 h and cooled at room temperature. Next, 70 mL of distilled water was poured into the mixture and was kept at 0–4 °C for 2 h. The creamy precipitated solids were filtered and washed with water and dried in air. The obtained powder was crystallized from ethanol to characterize yield 1.19 g, 80% of 1,4-bis (2-carboxyaldehyde phenoxy)butane. Anal. Calcd for  $\text{C}_{18}\text{H}_{18}\text{O}_4$ : C, 72.47; H, 6.08; Found: C, 72.1; H, 6.50; mp: 108 °C, IR (KBr,  $\text{cm}^{-1}$ ): 1678 [ $\nu(\text{C}=\text{O})$ ], 2956, 2862 [ $\nu(\text{aliphatic C-H})$ ].  $^1\text{H}$ NMR (400 MHz,  $\text{CDCl}_3$ ): 10.52 (s, 2H,  $\text{CH}=\text{O}$ ), 7–7.80 (m, 8H, aromatic), 4.2 (t, 4H, aliphatic  $\text{O}-\text{CH}_2-\text{C}$ ), 2.1 (t, 4H,  $\text{C}-\text{CH}_2-\text{C}$ ) (supporting information, Fig. S1).

### 2.4. Preparation of $\text{Fe}_3\text{O}_4@\text{SiO}_2-(\text{CH}_2)_3-\text{PBSB}$

A solution of 1,4-bis(2-carboxyaldehyde phenoxy)butane (1.49 g, 5 mol, in 60 mL of ethanol) was added to  $\text{Fe}_3\text{O}_4@\text{SiO}_2-(\text{CH}_2)_3\text{NH}_2$  (1.0 g in 60 mL of ethanol) suspension. The reaction mixture was refluxed by stirring for 2 days. After cooling the mixture,  $\text{Fe}_3\text{O}_4@\text{SiO}_2-(\text{CH}_2)_3-\text{PBSB}$  was separated using the external magnet and washed several times with water and ethanol, IR (KBr,  $\text{cm}^{-1}$ ): 623 [ $\nu(\text{Fe}-\text{O})$ ], 994 [ $\nu(\text{Si}-\text{O})$ ], 1636 [ $\nu(\text{imine})\text{C}=\text{N}$ ], 2925, 2849 [ $\nu(\text{aliphatic})\text{C-H}$ ], 3418 [ $\nu(\text{O}-\text{H})$ ].

### 2.5. Preparation of $\text{Fe}_3\text{O}_4@\text{SiO}_2-(\text{CH}_2)_3-\text{PBSB/MoO}_2$

345.2 g (1 mmol) of  $\text{MoO}_2\text{Cl}_2(\text{DMF})_2$  (prepared by the method given in the literature [50]) dissolved in 40 mL of dichloromethane was added dropwise to the suspension containing 1 g of  $\text{Fe}_3\text{O}_4@\text{SiO}_2-(\text{CH}_2)_3-\text{PBSB}$  in 40 mL of methanol, and the mixture was refluxed for a day. Then, the solid was separated using the external magnetic field and washed several times with water and ethanol to remove the unreacted  $\text{MoO}_2\text{Cl}_2(\text{DMF})_2$  and dried at 40 °C. IR (KBr,  $\text{cm}^{-1}$ ): 588 [ $\nu(\text{Fe}-\text{O})$ ], 916, 946 [ $\nu(\text{cis}, \text{O}=\text{Mo}=\text{O})$ ], 1024 [ $\nu(\text{Si}-\text{O}-\text{Si})$ ], 1652 [ $\nu(\text{C}=\text{N})$ ], 2938, 2860 [aliphatic,  $\text{C}-\text{H}$ ], 3410 [ $\nu(\text{O}-\text{H})$ ].

### 2.6. Studies of catalytic activity

The catalytic activity of heterogeneous  $\text{Fe}_3\text{O}_4@\text{SiO}_2-(\text{CH}_2)_3-\text{PBSB/MoO}_2$  catalyst was evaluated by the oxidation of various sulfides [methyl phenyl sulfide, diphenyl sulfide, benzyl phenyl sulfide, dipropyl sulfide, dibutyl sulfide, dimethyl sulfide, bis (4-hydroxyphenyl) sulfide, diallyl sulfide, and benzothiophene]. For testing catalytic oxidation activity, 0.0008 g ( $3.8 \times 10^{-4}$  mol) of  $\text{Fe}_3\text{O}_4@\text{SiO}_2-(\text{CH}_2)_3-\text{PBSB/MoO}_2$ , sulfides (10 mmol) and  $\text{H}_2\text{O}_2$  (30%) (10 mmol) were added in a ratio of 1:1 to the catalytic reactor. The catalytic system was mixed by stirring for 3 min, the catalyst was removed by the external magnetic field, and the oxidation products were monitored through GC.

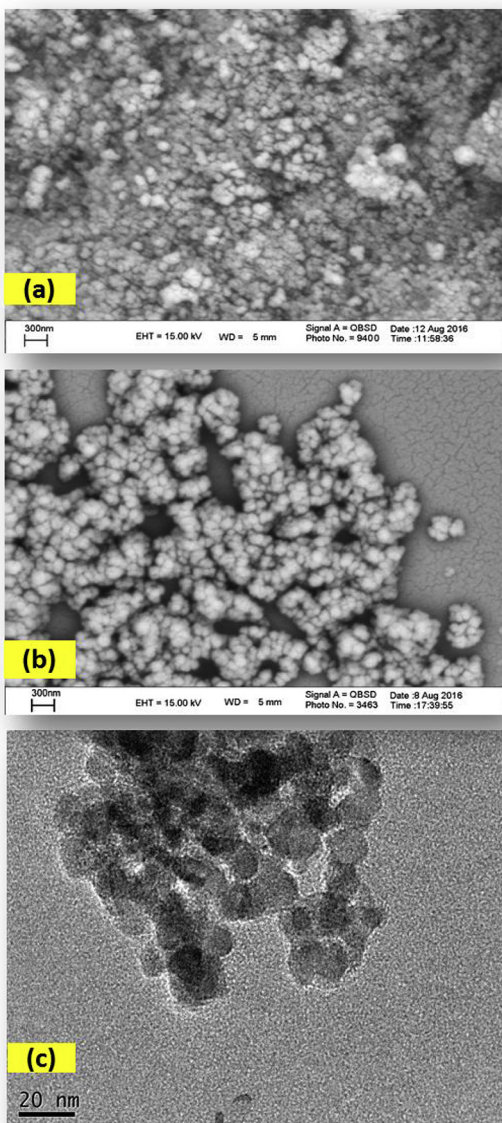


**Fig. 4.** Scanning electron microscopy images of (a) magnetite NPs, (b)  $\text{Fe}_3\text{O}_4@\text{SiO}_2-(\text{CH}_2)_3-\text{PBSB}/\text{MoO}_2$ , and transmission electron microscopy images of (c)  $\text{Fe}_3\text{O}_4@\text{SiO}_2-(\text{CH}_2)_3-\text{PBSB}/\text{MoO}_2$ .

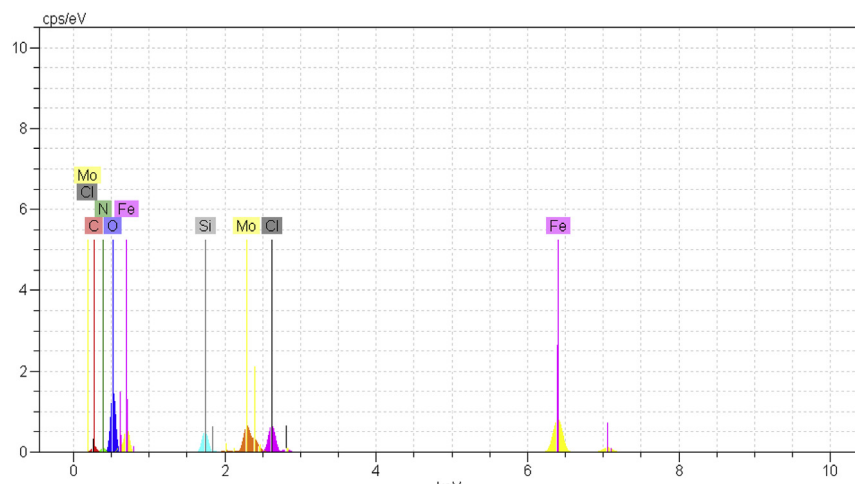


**Fig. 5.** EDX spectrum of  $\text{Fe}_3\text{O}_4@\text{SiO}_2-(\text{CH}_2)_3-\text{PBSB}/\text{MoO}_2$ .

### 3. Results and discussion

#### 3.1. Synthesis and characterization

Heterogeneous  $\text{Fe}_3\text{O}_4@\text{SiO}_2-(\text{CH}_2)_3-\text{PBSB}/\text{MoO}_2$  catalyst was prepared according to procedures shown in **Scheme 1** using a reaction of 1,4-bis(2-carboxyaldehyde phenoxy) butane,  $\text{MoO}_2\text{Cl}_2(\text{DMF})_2$ , and amino-modified  $\text{Fe}_3\text{O}_4@\text{SiO}_2$ NPs. **Fig. 1** indicates the FT-IR vibration of  $\text{Fe}_3\text{O}_4$  NP (**Fig. 1a**),  $\text{Fe}_3\text{O}_4@\text{SiO}_2-(\text{CH}_2)_3\text{NH}_2$  (**Fig. 1b**), supporting Schiff base ligand (**Fig. 1c**), and  $\text{Fe}_3\text{O}_4@\text{SiO}_2-(\text{CH}_2)_3-\text{PBSB}/\text{MoO}_2$  (**Fig. 1d**).  $\text{FeO}$  and  $\text{SiO}$  stretching bands appeared at 610 and  $998\text{ cm}^{-1}$ . As shown in **Fig. 1c** and d, the assigned band to  $\text{C}=\text{N}$  stretching vibration of supporting Schiff base ligand at  $1636\text{ cm}^{-1}$  has shifted to  $1652\text{ cm}^{-1}$  after coordination with  $\text{Mo}^{6+}$  center [51]. Hence, the appearance of

two adjacent bands at 916 and  $946\text{ cm}^{-1}$  indicates the presence of  $\text{MoO}_2$  group (**Fig. 1d**) [52]. The existence of bands at about  $2900\text{ cm}^{-1}$  can be assigned to aliphatic group ( $\text{CH}_2$ ) of APTMS. Considering all vibrations of IR spectra confirms the supporting of Schiff base  $\text{Mo}(\text{VI})$  complex on the magnetic NPs. **Fig. 2** shows the XRD pattern of  $\text{Fe}_3\text{O}_4$  NP (a) and  $\text{Fe}_3\text{O}_4@\text{SiO}_2-(\text{CH}_2)_3-\text{PBSB}/\text{MoO}_2$  (b). The comparison of two patterns (**Fig. 2a** and b) and those of standard  $\text{Fe}_3\text{O}_4$  NPs (reference JCPDS card no. 87-2334) demonstrated diffraction peaks for  $\text{Fe}_3\text{O}_4$  NPs and  $\text{Fe}_3\text{O}_4@\text{SiO}_2-(\text{CH}_2)_3-\text{PBSB}/\text{MoO}_2$ . The observed broad peak (about  $2\theta = 22-29^\circ$ ) of  $\text{Fe}_3\text{O}_4@\text{SiO}_2-(\text{CH}_2)_3\text{NH}_2$  and  $\text{Fe}_3\text{O}_4@\text{SiO}_2-(\text{CH}_2)_3-\text{PBSB}/\text{MoO}_2$  was assigned to the existence of amorphous silicon dioxide. **Fig. 3** shows the magnetization properties of synthesized  $\text{Fe}_3\text{O}_4$  NPs and  $\text{Fe}_3\text{O}_4@\text{SiO}_2-(\text{CH}_2)_3-\text{PBSB}/\text{MoO}_2$ . The magnetization plots

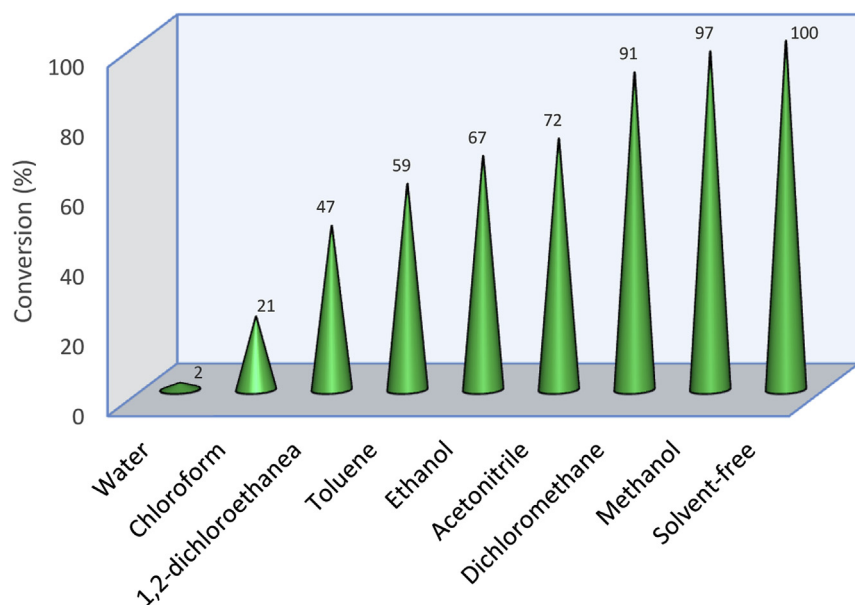


**Fig. 6.** Oxidation of thioanisole (1 mmol) in various solvents (5 mL) and under solvent-free conditions with 30%  $\text{H}_2\text{O}_2$  (1 mmol) and catalyst ( $3.8 \times 10^{-4}$  mmol) during 3 min.

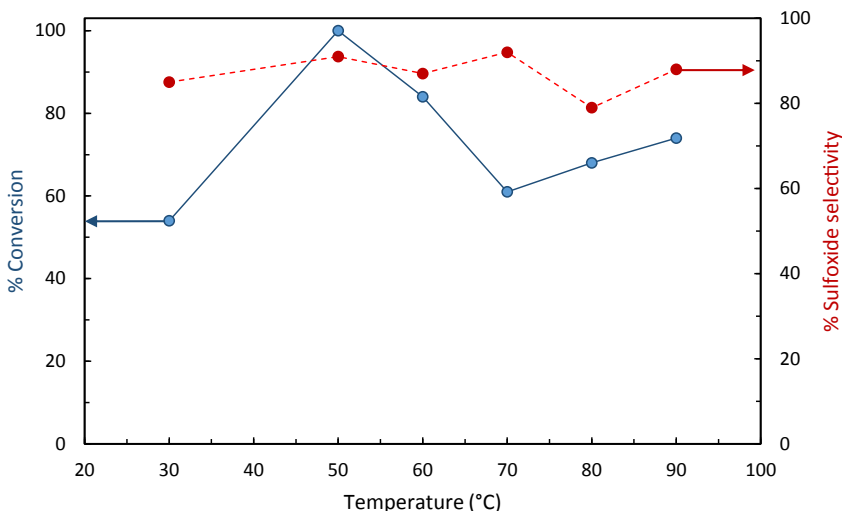


**Fig. 7.** Optimization of catalytic reaction temperature, thioanisole (1 mmol), 30% H<sub>2</sub>O<sub>2</sub> (1 mmol), catalyst ( $3.8 \times 10^{-4}$  mmol), solvent-free conditions, 3 min.

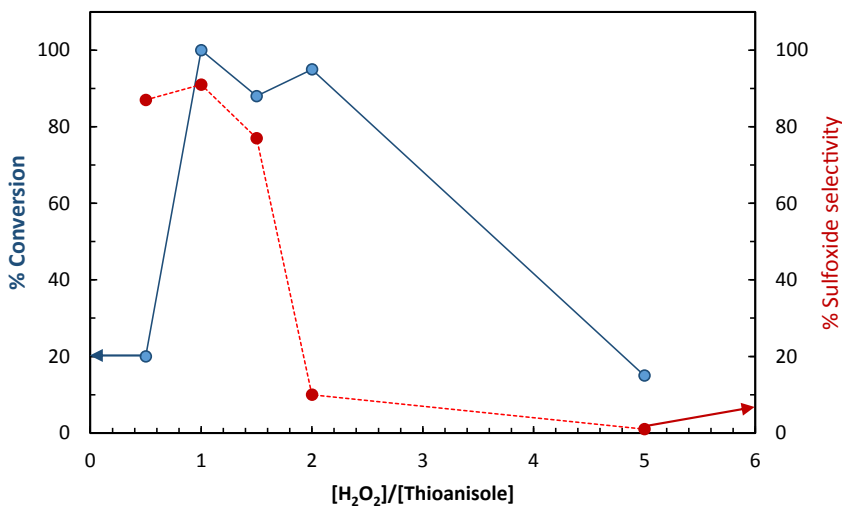


**Fig. 8.** Effect of a [H<sub>2</sub>O<sub>2</sub>]/[thioanisole] ratio on sulfoxidation conversion (left axis) and sulfoxidation selectivity (right axis), catalyst ( $3.8 \times 10^{-4}$  mmol), solvent-free conditions, 3 min, 50 °C.

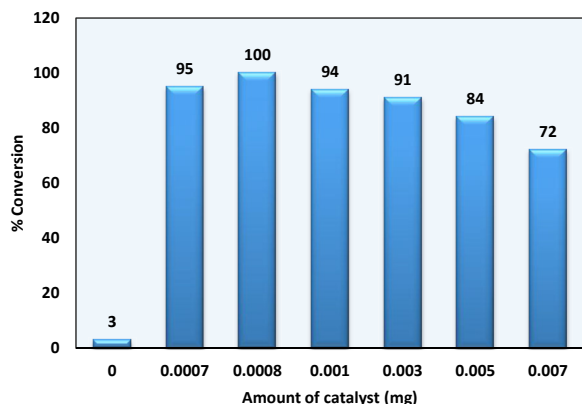


**Fig. 9.** Effect of a catalyst amount on sulfoxidation conversion under solvent-free conditions, thioanisole (10 mmol), H<sub>2</sub>O<sub>2</sub> (10 mmol), T = 50 °C, reaction time = 3 min.

**Table 1**  
Results of catalytic oxidation of various sulfides with H<sub>2</sub>O<sub>2</sub> (30% aqueous) catalyzed by Fe<sub>3</sub>O<sub>4</sub>@SiO<sub>2</sub>-(CH<sub>2</sub>)<sub>3</sub>-PBSB/MoO<sub>3</sub>.<sup>a</sup>

Sulfides	Sulfide (mmol)	% Conversion <sup>b</sup>	TOF (h <sup>-1</sup> ) <sup>c</sup>
<chem>C=C=S</chem>	10	100	526,000
<chem>CC=C=S</chem>	10	100	526,000
<chem>CCCCS</chem>	10	99<	<521,000
<chem>CCCCSC</chem>	10	95	500,000
<chem>c1ccc2c(c1)sc2</chem>	1	2	1052

**Table 1** (continued)

Sulfides	Sulfide (mmol)	% Conversion <sup>b</sup>	TOF (h <sup>-1</sup> ) <sup>c</sup>
<chem>C=Cc1ccccc1Sc2ccccc2</chem>	1	12	6300
<chem>C=Cc1ccccc1Sc2ccccc2</chem>	1	20	10,520
<chem>Oc1ccc(cc1)Sc2ccccc2</chem>	1	15	7890

<sup>a</sup> Catalytic reaction condition: solvent free; [sulfides]/[H<sub>2</sub>O<sub>2</sub>] (1:1), catalyst = 0.00038 mmol, reaction temperature = 50 °C, reaction time = 3 min.

<sup>b</sup> Conversion were determined by GC-FID (flame ionization detector), conversion = [(mole of SO) + (mole of SO<sub>2</sub>)]/(mole of initial sulfide).

<sup>c</sup> Calculated as (mmol of product)/(mmol of catalyst) × hours.

of Fe<sub>3</sub>O<sub>4</sub> NPs and Fe<sub>3</sub>O<sub>4</sub>@SiO<sub>2</sub>-(CH<sub>2</sub>)<sub>3</sub>-PBSB/MoO<sub>2</sub> reveal no hysteresis loop and have the magnetic saturation at 57.67 and 13.63 emu/g, respectively. It seems that the silica layer on magnetite NPs in Fe<sub>3</sub>O<sub>4</sub>@SiO<sub>2</sub>-(CH<sub>2</sub>)<sub>3</sub>-PBSB/MoO<sub>2</sub> is the leading cause of decreased magnetic saturation. However, the result suggests that the catalyst can be separated from the solution using the external magnetic field. Fig. 4a and b presents the SEM image of Fe<sub>3</sub>O<sub>4</sub> NPs and Fe<sub>3</sub>O<sub>4</sub>@SiO<sub>2</sub>-(CH<sub>2</sub>)<sub>3</sub>-PBSB/MoO<sub>2</sub>. The comparison of SEM images showed no change in morphology. Fig. 4c shows transmission electron microscopy images of the Fe<sub>3</sub>O<sub>4</sub>@SiO<sub>2</sub>-(CH<sub>2</sub>)<sub>3</sub>-PBSB/MoO<sub>2</sub> nanocatalyst, which is approximately 15–18 nm in size. As presented in Fig. 5, EDX of Fe<sub>3</sub>O<sub>4</sub>@SiO<sub>2</sub>-(CH<sub>2</sub>)<sub>3</sub>-PBSB/MoO<sub>2</sub> provides the existence of Mo, Si, C, Cl, and the other elements on the catalyst surface.

The thermal stability of the catalyst was studied using thermogravimetric assay. Given the thermogravimetric analysis in Fig. S2, the weight loss at 125 and 413 °C for Fe<sub>3</sub>O<sub>4</sub>@SiO<sub>2</sub>-(CH<sub>2</sub>)<sub>3</sub>-PBSB/MoO<sub>2</sub> can be attributed to the water removal and onset of molybdenum complex decomposition.

### 3.2. Catalytic oxidation of sulfides by Fe<sub>3</sub>O<sub>4</sub>@SiO<sub>2</sub>-(CH<sub>2</sub>)<sub>3</sub>-PBSB/MoO<sub>2</sub>

The Fe<sub>3</sub>O<sub>4</sub>@SiO<sub>2</sub>-(CH<sub>2</sub>)<sub>3</sub>-PBSB/MoO<sub>2</sub> catalyst was used to oxidize various sulfides using 30% H<sub>2</sub>O<sub>2</sub>. In the beginning of the catalytic process, some parameters were optimized, including the kind of solvent, amount of the catalyst, temperature of the catalytic reactor, reaction time, and substrate to oxidant molar ratio. After running the catalytic process for thioanisole oxidation with 30% H<sub>2</sub>O<sub>2</sub> and various solvents (5 mL), it has been found that solvent-free conditions bring about the highest conversion (100%) in 3 min (Fig. 6). Fig. 7 shows that the best conversion of thioanisole to oxidation products was obtained at 50 °C. The thioanisole was oxidized by several [H<sub>2</sub>O<sub>2</sub>]/[thioanisole] ratios. For this purpose, the 0.5, 1, 1.5, 2 ratios were set in the separate catalytic reactions. According to Fig. 8, the best sulfoxidation result was obtained in the ratio of 1:0 [H<sub>2</sub>O<sub>2</sub>]/[thioanisole]. Our results suggested that sulfone product was increased by rising the [H<sub>2</sub>O<sub>2</sub>]/[thioanisole] ratio more than 1:0. The catalyst level was optimized for thioanisole oxidation using 0.0, 0.0007, 0.0008, 0.001, 0.003, 0.005, 0.007 g of Fe<sub>3</sub>O<sub>4</sub>@SiO<sub>2</sub>-(CH<sub>2</sub>)<sub>3</sub>-PBSB/MoO<sub>2</sub>. As illustrated in Fig. 9, the optimal amount of the catalyst was reported as 0.0008 g. It appears that by increasing the catalyst amount more than 0.0008 g caused the decomposition of H<sub>2</sub>O<sub>2</sub>. Finally, we selected the sulfides (10 mmol) as substrate, 30% H<sub>2</sub>O<sub>2</sub> (10 mmol) as oxidant, and 0.0008 g

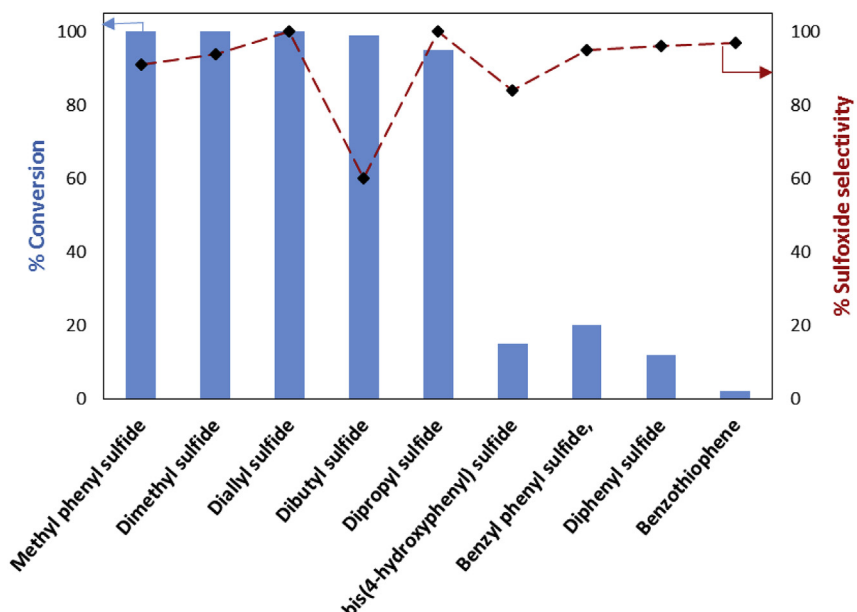


**Fig. 10.** Conversion and selectivity for oxidation of sulfides by the catalyst, solvent-free conditions, H<sub>2</sub>O<sub>2</sub> (30%), 50 °C, 3 min.

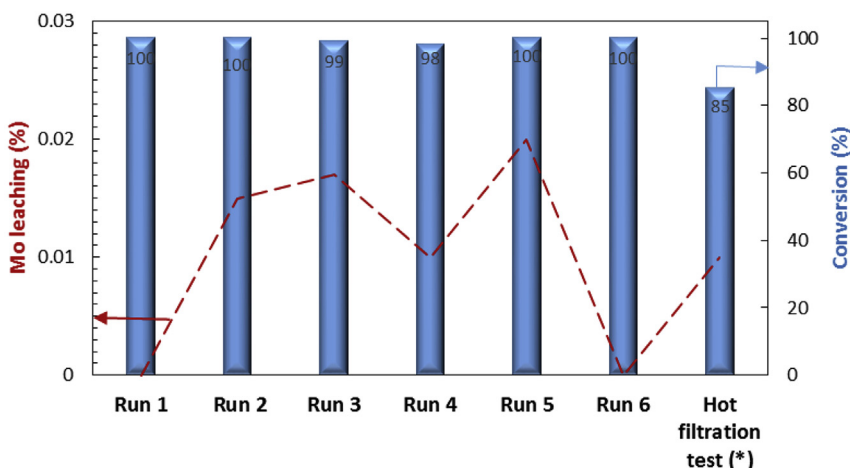


**Fig. 11.** Running of the catalyst several times, reaction conditions: solvent-free; thioanisole (10 mmol), H<sub>2</sub>O<sub>2</sub> (10 mmol), catalyst ( $3.8 \times 10^{-4}$  mmol), 3 min, 50 °C.  
\*Hot filtration test: after 1 min, the catalyst was removed from the reaction mixture (83% conversion) and the conversion was calculated after next 6 min (85% conversion).

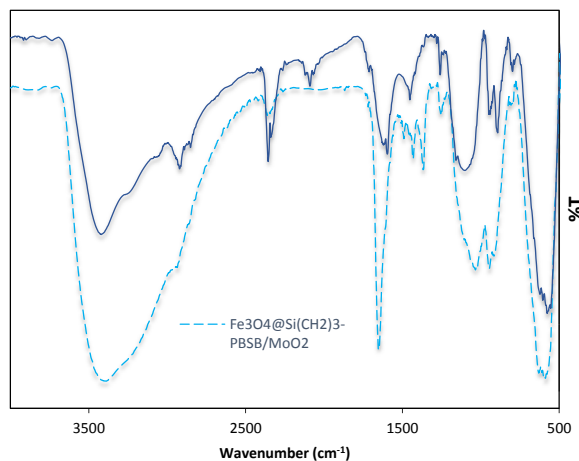


**Fig. 12.** FT-IR spectrum of  $\text{Fe}_3\text{O}_4@\text{SiO}_2-(\text{CH}_2)_3-\text{PBSB}/\text{MoO}_2$  before the catalytic reaction (solid line) and after the sixth run (dashed line).

of the catalyst ( $3.8 \times 10^{-4}$  mmol determined by atomic absorption spectroscopy) at 50 °C by stirring under solvent-free conditions for 3 min. The catalyst reactor monitoring exhibited no color and Mo leaching (detected by atomic absorption spectroscopy) in the final solution after the catalytic procedure. The results of catalytic oxidation of sulfides, methyl phenyl sulfide, diphenyl sulfide, benzyl phenyl sulfide, dipropyl sulfide, dibutyl sulfide, dimethyl sulfide, bis(4-hydroxyphenyl) sulfide, diallyl sulfide, and benzothiophene, are summarized in Table 1. Our results demonstrated 100% conversion for thioanisole, dimethyl sulfide, and diallyl sulfide, as well as <99% conversion for dibutyl sulfide in 3 min. Therefore, excellent turnover frequency of the catalyst was achieved to oxidize the thioanisole (526,000 h<sup>-1</sup>), dimethyl sulfide (526,000 h<sup>-1</sup>), diallyl sulfide (526,000 h<sup>-1</sup>), dibutyl sulfide (521,000 h<sup>-1</sup>), and dipropyl sulfide (500,000 h<sup>-1</sup>). Accordingly, the reason for low oxidation conversion of bis(4-hydroxyphenyl) sulfide, diphenyl sulfide, benzyl phenyl sulfide, and

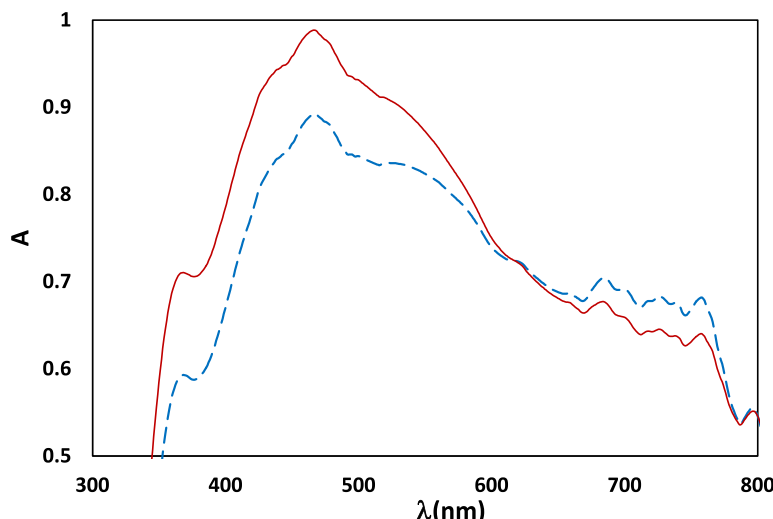


**Fig. 13.** DRS spectrum of  $\text{Fe}_3\text{O}_4@\text{SiO}_2-(\text{CH}_2)_3-\text{PBSB}/\text{MoO}_2$  before the catalytic process (solid line) and after the sixth run (dashed line).

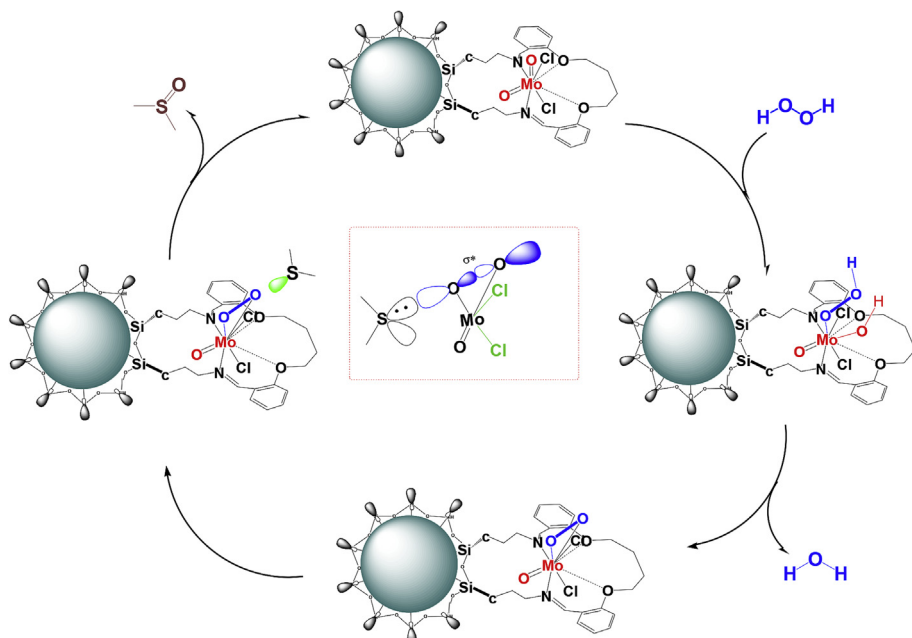
**Table 2**

Comparison of literature reports on the oxidation of thioanisole under various conditions.

Catalyst	Oxidant	Solvent	Time	%Conversion	Ref.
SBA-15 + ImCl + MoO <sub>5</sub>	H <sub>2</sub> O <sub>2</sub> (30%)	Methanol	60 min	95	[14]
TiO <sub>2</sub> /AA/MoO <sub>2</sub>	H <sub>2</sub> O <sub>2</sub> (30%)	Ethanol	30 min	100	[60]
[(n-C <sub>4</sub> H <sub>9</sub> ) <sub>4</sub> N]4(α-Mo <sub>8</sub> O <sub>26</sub> )	H <sub>2</sub> O <sub>2</sub> (30%)	Methanol	10 min	98	[64]
ML <sub>2</sub> (Cu, Co Zn, Pd)	H <sub>2</sub> O <sub>2</sub> (30%)	Solvent-free	180 min	80	[55]
Ti-MCM-41	H <sub>2</sub> O <sub>2</sub> (30%)	Solvent-free	120 min	89	[56]
[PO <sub>4</sub> (WO(O <sub>2</sub> ) <sub>3</sub> ) <sub>4</sub> ]@PIILP	H <sub>2</sub> O <sub>2</sub> (30%)	Methanol	15 min	95	[62]
[MRAMoO <sub>2</sub> (O <sub>2</sub> )]	H <sub>2</sub> O <sub>2</sub> (30%)	Methanol	15 min	99	[63]
VO-2A3HP-MCM-41	H <sub>2</sub> O <sub>2</sub> (30%)	Solvent-free	120 min	96	[57]
Ti-IEZ-MWW	H <sub>2</sub> O <sub>2</sub> (30%)	Solvent-free	120 min	<99	[58]
Fe <sub>3</sub> O <sub>4</sub> @chit-based Cu complex	H <sub>2</sub> O <sub>2</sub> (30%)	Solvent-free	90 min	97	[54]
p-TsOH	H <sub>2</sub> O <sub>2</sub> (30%)	Solvent-free	85 min	90	[59]
e3O <sub>4</sub> @APTMS/fluorene-SBeMoO <sub>2</sub>	H <sub>2</sub> O <sub>2</sub> (30%)	Solvent-free	5 min	99	[61]
Fe <sub>3</sub> O <sub>4</sub> @Si-APFSB-MoO <sub>2</sub>	H <sub>2</sub> O <sub>2</sub> (30%)	Solvent-free	3 min	100	This work

benzothiophene is related to the steric effect of sulfides and the catalyst. The selectivity of oxidation reactions for sulfoxide production is in the acceptable ranges (Fig. 10). The catalytic oxidation of the substrate with aqueous H<sub>2</sub>O<sub>2</sub> in the blank run (without catalysts) occurs with 2% conversion. The chemical and physical stabilities of the catalyst result in recycling and reusing of the catalyst several times (six times). As shown in Fig. 11, the catalyst was separated easily with the magnet and used several times for epoxidation process. A hot filtration test was performed for

further investigations of catalyst leaching. For this purpose, the catalyst was removed from the reaction mixture after 1 min and the conversion was calculated after the other 3 min. The conversion showed no significant increase. Fig. 12 presents no change in the IR spectra for the catalyst before oxidation and sixth run. Therefore, comparison between DRS spectra of the catalyst (Fig. 13) before and after the oxidation process shows no change. Regarding the conversion results and literature [53], the proposed mechanism seems to be followed through a seven-

**Scheme 2.** Proposed catalytic cycle for oxidation of sulfides by Fe<sub>3</sub>O<sub>4</sub>@SiO<sub>2</sub>-(CH<sub>2</sub>)<sub>3</sub>-PBSB/MoO<sub>2</sub> with H<sub>2</sub>O<sub>2</sub>.

coordinate intermediate (**Scheme 2**). In a catalytic cycle, oxidation process starts with attacking of  $\text{H}_2\text{O}_2$  to Mo center and generation of oxo–peroxo Mo(VI) precursor. In the following, sulfur electron pair attacks the  $\sigma^*(\text{O}-\text{O})$  of oxo–peroxo Mo(VI), and the catalyst is regenerated with production of sulfoxide.

**Table 2** shows the comparison between the novel presented catalyst and literature reports. The  $\text{Fe}_3\text{O}_4@\text{SiO}_2-(\text{CH}_2)_3-\text{PBSB}/\text{MoO}_2$  indicated higher oxidation catalytic activity of thioanisole with excellent TOF (TOF: turnover frequency) (<526,000  $\text{h}^{-1}$ ). Finally, by comparing the catalytic reaction time of the reported works in the literature (**Table 2**), 90 min [54], 180 min [55], 120 min [56–58], 60 min [14], 85 min [59], 30 min [60,61], and 15 min [62,63] with  $\text{Fe}_3\text{O}_4@\text{SiO}_2-(\text{CH}_2)_3-\text{PBSB}/\text{MoO}_2$  (3 min), it is found that the presented catalyst is efficient, time saving, and paramount.

#### 4. Conclusions

In the present study, following our previous researches on the catalytic activity, we found successful covalent anchoring of a phenoxy butane-based Mo(VI) tetradeятate Schiff base complex on magnetite NPs. The novel paramagnetic recoverable catalyst has been studied as nanocatalyst for oxidation of methyl phenyl sulfide, diphenyl sulfide, benzyl phenyl sulfide, dipropyl sulfide, dibutyl sulfide, dimethyl sulfide, bis(4-hydroxyphenyl) sulfide, diallyl sulfide, and benzothiophene. The catalyst was recovered successfully using the magnet from the catalytic reactor and reused as a catalyst for six times without decrease in conversion and selectivity.  $\text{Fe}_3\text{O}_4@\text{SiO}_2-(\text{CH}_2)_3-\text{PBSB}/\text{MoO}_2$  catalyst illustrated excellent catalytic activity and remarkable short catalytic time (3 min) than the other reported catalysts. The  $\text{Fe}_3\text{O}_4@\text{SiO}_2-(\text{CH}_2)_3-\text{PBSB}/\text{MoO}_2$  catalyst indicated a remarkable high TOF (<526,000  $\text{h}^{-1}$ ).

#### Acknowledgments

The authors would like to thank and appreciate Research Deputy of Mohaghegh-e-Ardabili University, Iran, for financial support under the project (Grant number: 281).

#### Appendix A. Supplementary data

Supplementary data related to this article can be found at <http://dx.doi.org/10.1016/j.crci.2017.07.004>.

#### References

- [1] O.A. Wong, Y. Shi, *Chem. Rev.* 108 (2008) 3958–3987.
- [2] C.A. Gamelas, A.C. Gomes, S.M. Bruno, F.A. Almeida Paz, A.A. Valente, M. Pillinger, C.C. Romão, I.S. Gonçalves, *Dalton Trans.* 41 (2012) 3474–3484.
- [3] F. Bigi, H.Q. Nimal Gunaratne, C. Quarantelli, K.R. Seddon, *C. R. Chimie* 14 (2011) 685–687.
- [4] B.B. Loura, T.G. Alhazov, O. Fioletova, N.S. Amirkouliane, *C. R. Chimie* 7 (2004) 45–50.
- [5] S. Menati, H. Amiri Rudbari, B. Askari, M. Riahi Farsani, F. Jalilian, G. Dini, *C. R. Chimie* 19 (2016) 346–355.
- [6] N. Baig, V.K. Madduluri, A.K. Sah, *RSC Adv.* 6 (2016) 28015–28022.
- [7] A. Rostami, B. Tahmasbi, F. Abedi, Z. Shokri, *J. Mol. Catal. A: Chem.* 378 (2013) 200–205.
- [8] M. Madesclaire, *Tetrahedron* 42 (1986) 5459–5495.
- [9] A.R. Supale, G.S. Gokavi, *Catal. Lett.* 124 (2008) 284–287.
- [10] M. Bagherzadeh, M. Zare, *J. Sulfur Chem.* 32 (2011) 335–343.
- [11] K. Krishnasamy, V. Venkateswaran, M. Shanmugam, J. Dharmaraja, *J. Sulfur Chem.* 28 (2007) 365–369.
- [12] M. Rahimizadeh, M. Bakavoli, H. Hassani, M. Gholizadeh, *J. Sulfur Chem.* 28 (2007) 265–268.
- [13] A. Basak, A.U. Barlan, H. Yamamoto, *Tetrahedron: Asymmetry* 17 (2006) 508–511.
- [14] C.J. Carrasco, F. Montilla, L. Bobadilla, S. Ivanova, J.A. Odriozola, A. Galindo, *Catal. Today* 255 (2015) 102–108.
- [15] M. Bagherzadeh, M.M. Haghdoost, A. Ghanbarpour, M. Amini, H.R. Khavasi, E. Payab, A. Ellern, L.K. Woo, *Inorg. Chim. Acta* 411 (2014) 61–66.
- [16] N. Gharah, S. Chakraborty, A.K. Mukherjee, R. Bhattacharyya, *Inorg. Chim. Acta* 362 (2009) 1089–1100.
- [17] A. Fuerte, M. Iglesias, F. Sánchez, A. Corma, *J. Mol. Catal. A: Chem.* 211 (2004) 227–235.
- [18] M. Bagherzadeh, M. Zare, *J. Coord. Chem.* 66 (2013) 2885–2900.
- [19] A. Bezaatpour, S. Khatami, M. Amiri, *RSC Adv.* 6 (2016) 27452–27459.
- [20] A.K. Sah, N. Baig, *Catal. Lett.* 145 (2015) 905–909.
- [21] M.A. Martins, C.P. Frizzo, D.N. Moreira, L. Buriol, P. Machado, *Chem. Rev.* (Washington, DC, U. S.) 109 (2009) 4140–4182.
- [22] R. Noyori, M. Aoki, K. Sato, *Chem. Commun.* (Cambridge, U. K.) (2003) 1977–1986.
- [23] S. Caron, R.W. Dugger, S.G. Ruggeri, J.A. Ragan, D.H.B. Ripin, *Chem. Rev.* (Washington, DC, U. S.) 106 (2006) 2943–2989.
- [24] A. Podgorsek, M. Zupan, J. Iskra, *Angew. Chem., Int. Ed.* 48 (2009) 8424–8450.
- [25] R. Dileep, B. Rudresha, *RSC Adv.* 5 (2015) 65870–65873.
- [26] A. Mavrogiorgou, M. Baikousi, V. Costas, E. Mouzourakis, Y. Deligiannakis, M. Karakassis, M. Louloudi, *J. Mol. Catal. A: Chem.* 413 (2016) 40–55.
- [27] A. Bezaatpour, M. Amiri, V. Jahed, *J. Coord. Chem.* 64 (2011) 1837–1847.
- [28] L. Hamidipour, F. Farzaneh, *C. R. Chimie* 17 (2014) 927–933.
- [29] C. Baleizão, B. Gigante, D. Das, M. Álvaro, H. Garcia, A. Corma, *J. Catal.* 223 (2004) 106–113.
- [30] A. Bezaatpour, M. Behzad, V. Jahed, M. Amiri, Y. Mansoori, Z. Rajabali-zadeh, S. Sarvi, *Reac. Kinet. Mech. Cat.* 107 (2012) 367–381.
- [31] M. Fadhl, I. Khedher, J.M. Fraile, *J. Mol. Catal. A: Chem.* 420 (2016) 282–289.
- [32] S.P. Shylesh, M. Jia, A. Seifert, S. Adappa, S. Ernst, W.R. Thiel, *New J. Chem.* 33 (2009) 717–719.
- [33] A.M. García, V. Moreno, S.X. Delgado, A.E. Ramírez, L.A. Vargas, M.Á. Vicente, A. Gil, L.A. Galeano, *J. Mol. Catal. A: Chem.* 416 (2016) 10–19.
- [34] J. Zhang, P. Jiang, Y. Shen, W. Zhang, X. Li, *Microporous Mesoporous Mater.* 206 (2015) 161–169.
- [35] P. Piaggio, P. McMorn, C. Langham, D. Bethell, P.C. Bulman-Page, F.E. Hancock, G.J. Hutchings, *New J. Chem.* 22 (1998) 1167–1169.
- [36] T. Chattopadhyay, A. Chakraborty, S. Dasgupta, A. Dutta, M.I. Menéndez, E. Zangrando, *Appl. Organomet. Chem.* (2016), <http://dx.doi.org/10.1002/aoc.3663>.
- [37] P.B. Bhat, R.B. Bhat, *New J. Chem.* 39 (2015) 273–278.
- [38] A. Farokhi, H. Hosseini-Monfared, *New J. Chem.* 40 (2016) 5032–5043.
- [39] J. Sun, G. Yu, L. Liu, Z. Li, Q. Kan, Q. Huo, J. Guan, *Catal. Sci. Technol.* 4 (2014) 1246–1252.
- [40] M. Mohammadikish, M. Masteri-Farahani, S. Mahdavi, *J. Magn. Magn. Mater.* 354 (2014) 317–323.
- [41] T. Li, C. Yang, X. Rao, F. Xiao, J. Wang, X. Su, *Ceram. Int.* 41 (2015) 2214–2220.
- [42] C.I. Fernandes, M.D. Carvalho, L.P. Ferreira, C.D. Nunes, P.D. Vaz, *J. Organomet. Chem.* 760 (2014) 2–10.
- [43] X. Zhang, G. Wang, M. Yang, Y. Luan, W. Dong, R. Dang, H. Gao, J. Yu, *Catal. Sci. Technol.* 4 (2014) 3082–3089.
- [44] A. Bezaatpour, *Reac. Kinet. Mech. Cat.* 112 (2014) 453–465.
- [45] D.M. Boghaei, A. Bezaatpour, M. Behzad, *J. Mol. Catal. A: Chem.* 245 (2006) 12–16.
- [46] J. Rahchamani, M. Behzad, A. Bezaatpour, V. Jahed, G. Dutkiewicz, M. Kubicki, M. Salehi, *Polyhedron* 30 (2011) 2611–2618.
- [47] Z. Peng, K. Hidajat, M. Uddin, *J. Colloid Interface Sci.* 271 (2004) 277–283.
- [48] X. Huang, W. Guo, G. Wang, M. Yang, Q. Wang, X. Zhang, Y. Feng, Z. Shi, C. Li, *Mater. Chem. Phys.* 135 (2012) 985–990.

- [49] S. İlhan, H. Temel, A. Kılıç, J. Coord. Chem. 61 (2008) 277–284.
- [50] F.J. Arnaiz, R. Aguado, J. Sanz-Aparicio, M. Martínez-Ripoll, Polyhedron 13 (1994) 2745–2749.
- [51] W. Hill, N. Atabay, C. McAuliffe, F. McCullough, S. Razzoki, Inorg. Chim. Acta 35 (1979) 35–41.
- [52] J. Topich, Inorg. Chem. 20 (1981) 3704–3707.
- [53] M. Bagherzadeh, M.M. Haghdoost, M. Amini, P.G. Derakhshandeh, Catal. Commun. 23 (2012) 14–19.
- [54] A. Fakhri, A. Naghipour, Mater. Technol. 31 (2016) 846–853.
- [55] M. Khorshidifard, H.A. Rudbari, B. Askari, M. Sahihi, M.R. Farsani, F. Jalilian, G. Bruno, Polyhedron 95 (2015) 1–13.
- [56] Y. Kon, T. Yokoi, M. Yoshioka, Y. Uesaka, H. Kujira, K. Sato, T. Tatsumi, Tetrahedron Lett. 54 (2013) 4918–4921.
- [57] M. Nikoorazm, A. Ghorbani-Choghamarani, M. Khanmoradi, Appl. Organomet. Chem. 30 (2016) 236–241.
- [58] Y. Kon, T. Yokoi, M. Yoshioka, S. Tanaka, Y. Uesaka, T. Mochizuki, K. Sato, T. Tatsumi, Tetrahedron 70 (2014) 7584–7592.
- [59] A. Rostami, F. Hassanian, A. Ghorbani-Choghamarani, S. Saadati, Phosphorus, Sulfur Silicon Relat. Elem. 188 (2013) 833–838.
- [60] M. Jafarpour, A. Rezaeifard, M. Ghahramaninezhad, F. Feizpour, Green Chem. 17 (2015) 442–452.
- [61] A. Bezaatpour, E. Askarizadeh, S. Akbarpour, M. Amiri, B. Babaei, J. Mol. Catal. A: Chem. 436 (2017) 199–209.
- [62] S. Doherty, J.G. Knight, M.A. Carroll, J.R. Ellison, S.J. Hobson, S. Stevens, C. Hardacre, P. Goodrich, Green Chem. 17 (2015) 1559–1571.
- [63] J.J. Boruah, S.P. Das, S.R. Ankireddy, S.R. Gogoi, N.S. Islam, Green Chem. 15 (2013) 2944–2959.
- [64] C. Yang, Q. Jin, H. Zhang, J. Liao, J. Zhu, B. Yu, J. Deng, Green Chem. 11 (2009) 1401–1405.